Available online at www.sciencedirect.com
ScienceDirect
Journal of Sound and Vibration 319 (2009) 681–697
JOURNAL OF SOUND AND VIBRATION
www.elsevier.com/locate/jsvi

Free vibration analysis of ribbed plates by a combined analytical–numerical method

Lorenzo Dozio*, Massimo Ricciardi

Politecnico di Milano, Dipartimento di Ingegneria Aerospaziale, via La Masa, 34, 20156 Milano, Italy

Received 20 December 2007; received in revised form 21 May 2008; accepted 17 June 2008
Handling Editor: C.L. Morfey
Available online 6 August 2008

Abstract

An easy to code and computationally efficient analytical–numerical method for quick prediction of the modal characteristics of rectangular ribbed plates is presented. The approach is suitable for low-frequency free vibration analysis of thin rectangular plates reinforced by a small number of light stiffeners. The assumed-modes method is used to formulate the equations of motion of the plate and the rib separately. The motion of the built-up structure is then obtained by enforcing appropriate continuity conditions between the two. The resulting sparse generalized eigenvalue problem can be profitably solved by reliable methods to calculate only a small set of selected eigenmodes. An alternative formulation is also proposed for the single-ribbed case which leads to a compact analytical form of the frequency equation whose solution can be easily determined either graphically or numerically. The present method demonstrates good agreement with published results and standard finite element analysis.

1. Introduction

Structures consisting of thin plates stiffened by a set of beams form a class of structural elements of practical importance in various engineering applications, such as aircrafts and ships. Since aerospace and marine vehicles are subjected to dynamic loads, confident prediction of natural frequencies of a structural component is essential in preventing excessive vibration levels, which may result in fatigue failure or very high noise levels.

Introducing stiffeners to plates complicates the dynamic analysis and some simplifying assumptions have to be made in order to facilitate a solution of the problem. A huge amount of approximate analytical and numerical methods has been proposed to study the vibration of rib-stiffened plates, hence no attempt is made here to provide a complete review of the available procedures. Proposed approaches include the orthotropic [1] and grillage [2] models, the Lagrange multiplier formalism [3], the Rayleigh–Ritz method [4,5], the finite difference method [6], the finite element method [7–9], the differential quadrature method [10], and the meshless method [11]. Nowadays, with the help of high-speed computers, numerical methods such as the finite element method (FEM) are extensively adopted in industry due to their high accuracy and versatility.

*Corresponding author. Tel.: +39 02 2399 8329; fax: +39 02 2399 8334.
E-mail addresses: lorenzo.dozio@polimi.it, dozio@aero.polimi.it (L. Dozio).

0022-460X/$ - see front matter © 2008 Elsevier Ltd. All rights reserved.
doi:10.1016/j.jsv.2008.06.024

However, they are somewhat time-consuming for problems having simple geometry and boundary conditions and become inefficient for parametric and optimization studies during the preliminary design process. Simpler and faster models of catering for these problems are desirable.

The simplified formulation presented in this paper provides an approximate tool for fast prediction of the first natural frequencies and mode shapes of rectangular thin plates orthogonally reinforced by a small number of light eccentric stiffeners. Since narrow stiffeners are considered, they are treated as beams and the beam/plate interface is modeled as a nonslip line connection, i.e., the continuity of displacements and rotations is assumed between the plate and the beam. In addition, the present theory assumes pure bending deformation of the plate. As a result of the plate bending, the stiffening beams are subject to bending and torsion deformations. For eccentrically rib-stiffened plates, in-plane forces do come into play and the flexural and membrane action are *a priori* coupled. However, the in-plane contribution may be neglected when dealing with a small number of light stiffening beams and when the first few natural frequencies of the built-up structure are of interest [12,13]. Under the above assumptions, the eigenvalue problem of the dynamical system is obtained and solved by a combined analytical–numerical method similar to the approach used by Wu and Luo [14] and Cha [15]. Both the plate and beam motion is described separately by using the well-known assumed-modes method [16]. In the present case, the admissible functions for the plate are selected as the product of vibrating beam eigenfunctions of equivalent boundary conditions [17,18]. The motion of the combined system is obtained by enforcing appropriate continuity conditions between parts of the structures. It will be shown that the resulting mass and stiffness matrices are in a sparse form. The corresponding generalized sparse eigenproblem can be solved by reliable and efficient methods, such as Lanczos and Arnoldi-type algorithms, to obtain a small set of selected eigenpairs. Further, the sparsity of the eigenproblem is exploited to obtain a simple expression for the frequency equation of single-ribbed plates by using the matrix determinant lemma [19,20]. The zeros of the resulting frequency equation can be quickly determined either graphically or numerically by using any standard root solver routine. Numerical examples are presented to evaluate the accuracy of the proposed method. The calculated results compare well with those obtained using a standard FEM analysis and more refined models proposed by other researchers.

2. Formulation

2.1. Problem statement

Consider a thin, flat and rectangular plate, as shown in Fig. 1, of isotropic and linearly elastic material with modulus of elasticity E, Poisson ratio ν and density ρ, having uniform thickness h and occupying the region of the (x,y)-plane $\Omega(x,y): 0\leqslant x\leqslant a, 0\leqslant y\leqslant b$. The plate is orthogonally stiffened by a set of $i=1,2,\ldots,I$ prismatic beams parallel to the y-axis and a set of $j=1,2,\ldots,J$ prismatic beams parallel to the x-axis. Beams made of the same material as the plate are considered. The present theory assumes decoupling between in-plane and out-of-plane motion of the plate and only bending motion is considered. As a result of plate bending, the beams are subject to bending and torsion deformations. The plate is modeled using classical thin plate theory, i.e., the effects of shear deformation and rotary inertia are neglected. The stiffening beams are modeled as Euler–Bernoulli beams and the effects of restrained warping are included. The plate and beam motion are described separately by using the assumed-modes method. The governing equation of motion of each substructure is forced by the coupling loads at the beam/plate interface. The arising dynamic loads at the ith y-wise interface include a distribution of torsional line moment $m^i=m^i(y,t)$ and a transverse line force distribution $f^i=f^i(y,t)$. The arising dynamic loads at the jth x-wise interface include a distribution of torsional line moment $m^j=m^j(x,t)$ and a transverse line force distribution $f^j=f^j(x,t)$.

2.2. Plate

According to the classical theory of thin plates, the equation of motion of the forced plate is given as follows [21]:

$$D\nabla^4 w+\rho h\frac{\partial^2 w}{\partial t^2}=-\sum_{i=1}^{I}(f^i\delta_{xi}+m^i\delta'_{xi})-\sum_{j=1}^{J}(f^j\delta_{yj}+m^j\delta'_{yj}) \tag{1}$$

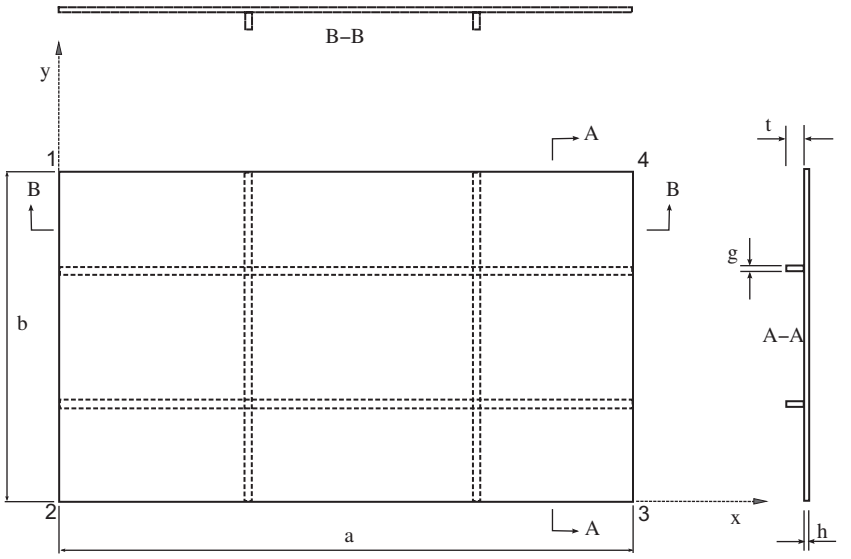

Fig. 1. Geometry of a rectangular plate orthogonally stiffened.

where $w = w(x, y, t)$ is the transverse displacement, $D = Eh^3/12(1 - \nu^2)$ is the flexural rigidity of the plate, ∇^4 is the biharmonic operator, $\delta_{xi} = \delta(x - x_i)$, $\delta_{yj} = \delta(y - y_j)$, where δ is the Dirac delta function, x_i denotes the location of the ith y-wise beam and y_j denotes the location of the jth x-wise beam. δ' represents the first derivative of the Dirac delta function with respect to its argument, i.e., $\delta'_{xi} = (\partial/\partial x)\delta(x - x_i)$ and $\delta'_{yj} = (\partial/\partial y)\delta(y - y_j)$. Using the assumed-modes method [16] and assuming a time-harmonic vibration, the plate deflection w can be expressed as the superposition of a finite number of mode shape functions $s_{mn}(x, y)$ as follows:

$$w = \sum_{m=1}^{M}\sum_{n=1}^{N} s_{mn}(x, y) w_{mn} e^{j\omega t} \tag{2}$$

where w_{mn} is the modal amplitude of the (m, n)th mode of the plate and ω is the circular frequency. The mode shape functions can be arbitrarily chosen as long as they satisfy at least the essential boundary conditions. For rectangular plates, the mode shape functions can be written as the product of two independent beam functions [17]:

$$s_{mn}(x, y) = \phi_m(x)\psi_n(y) \tag{3}$$

Following Warburton [18], the chosen form for the beam function used in the present study is

$$\phi_m(x) = A_m \cosh(\beta_m x) + B_m \cos(\beta_m x) + C_m \sinh(\beta_m x) + D_m \sin(\beta_m x), \tag{4}$$

where the constants A_m, B_m, C_m, D_m and β_m are determined according to the specified edge boundary conditions of the plate at $x = 0$ and a. The values for three different kinds of boundary conditions, i.e., simply supported–simply supported (SS), clamped–simply supported (CS), and clamped–clamped (CC), are listed in Table 1 as well as the characteristic equation governing the mated eigenvalue problem. The beam function $\psi_n(y)$ is defined accordingly to Eq. (4), where x and m are replaced by y and n and the constants A_n, B_n, C_n, D_n, and β_n are determined according to the boundary condition of the plate at the edges $y = 0$ and b. After substituting Eq. (2) into Eq. (1), multiplying it with the (p, q)th mode shape function, $s_{pq}(x, y) = \phi_p(x)\psi_q(y)$, and integrating over the area of the plate, the solutions must satisfy the following set

Table 1
Coefficients of beam functions $\phi_m(x)$

BCs	Characteristic equation	A_m	B_m	C_m	D_m
SS	$\sin(\beta a)=0$	0	0	0	1
CS	$\tan(\beta a)-\tanh(\beta a)=0$	1	−1	$-\dfrac{\cosh(\beta_m a)-\cos(\beta_m a)}{\sinh(\beta_m a)-\sin(\beta_m a)}$	$\dfrac{\cosh(\beta_m a)-\cos(\beta_m a)}{\sinh(\beta_m a)-\sin(\beta_m a)}$
CC	$\cos(\beta a)\cosh(\beta a)-1=0$	1	−1	$-\dfrac{\cosh(\beta_m a)-\cos(\beta_m a)}{\sinh(\beta_m a)-\sin(\beta_m a)}$	$\dfrac{\cosh(\beta_m a)-\cos(\beta_m a)}{\sinh(\beta_m a)-\sin(\beta_m a)}$

of $M \times N$ coupled equations:

$$\sum_{m=1}^{M}\sum_{n=1}^{N} w_{mn}\int_0^a\int_0^b [D(\phi_m''''\psi_n\phi_p\psi_q + 2\phi_m''\psi_n''\phi_p\psi_q + \phi_m\psi_n''''\phi_p\psi_q) - \rho h\omega^2\phi_m\psi_n\phi_p\psi_q]\,\mathrm{d}x\,\mathrm{d}y$$
$$= -\sum_{i=1}^{I}\int_0^a\int_0^b [f^i\delta_{xi}\phi_p\psi_q + m^i\delta'_{xi}\phi_p\psi_q]\,\mathrm{d}x\,\mathrm{d}y - \sum_{j=1}^{J}\int_0^a\int_0^b [f^j\delta_{yj}\phi_p\psi_q + m^j\delta'_{yj}\phi_p\psi_q]\,\mathrm{d}x\,\mathrm{d}y \tag{5}$$

where the prime denotes derivative of the shape function with respect to its argument, i.e., $\phi'_m = \partial\phi_m/\partial x$, $\psi'_n = \partial\psi_n/\partial y$. Using the one dominant beam function for the (m,n)th mode (the so-called single-term solution [17,18]), Eq. (5) can be approximated as follows:

$$[D(I_{1m}I_{2n} + 2I_{3m}I_{4n} + I_{6m}I_{5n}) - \rho h\omega^2 I_{6m}I_{2n}]w_{mn} = f_{mn} + m_{mn} \tag{6}$$

where $m = 1,2,\ldots,M$ and $n = 1,2,\ldots,N$, and f_{mn} and m_{mn} are the modal coupling line forces and moments, respectively, given by

$$f_{mn} = -\sum_{i=1}^{I}\phi_m^{x_i}\int_0^b f^i\psi_n\,\mathrm{d}y - \sum_{j=1}^{J}\psi_n^{y_j}\int_0^a f^j\phi_m\,\mathrm{d}x \tag{7}$$

$$m_{mn} = -\sum_{i=1}^{I}\phi_m'^{x_i}\int_0^b m^i\psi_n\,\mathrm{d}y - \sum_{j=1}^{J}\psi_n'^{y_j}\int_0^a m^j\phi_m\,\mathrm{d}x \tag{8}$$

where the superscripts x_i, y_j denote the location where the corresponding shape function is evaluated, i.e., $\phi_m^{x_i} = \phi_m(x_i)$, $\psi_n^{y_j} = \psi_n(y_j)$. Eq. (6) can be written in more compact notation as

$$(\kappa_{mn} - \omega^2\mu_{mn})w_{mn} = f_{mn} + m_{mn} \tag{9}$$

where κ_{mn} is the modal stiffness of the (m,n)th mode calculated as follows:

$$\kappa_{mn} = D(I_{1m}I_{2n} + 2I_{3m}I_{4n} + I_{6m}I_{5n}) \tag{10}$$

and μ_{mn} is the modal mass of the (m,n)th mode expressed as

$$\mu_{mn} = \rho h I_{6m}I_{2n} \tag{11}$$

In Eqs. (6), (10), and (11), I_{1-6} are the following definite integrals:

$$I_{1m} = \int_0^a \phi_m''''\phi_m\,\mathrm{d}x, \quad I_{4n} = \int_0^b \psi_n''\psi_n\,\mathrm{d}y$$
$$I_{2n} = \int_0^b \psi_n^2\,\mathrm{d}y, \quad I_{5n} = \int_0^b \psi_n''''\psi_n\,\mathrm{d}y$$
$$I_{3m} = \int_0^a \phi_m''\phi_m\,\mathrm{d}x, \quad I_{6m} = \int_0^a \phi_m^2\,\mathrm{d}x \tag{12}$$

According to the single-term solution, the approximate natural frequency of the (m,n)th plate mode is given by

$$\omega_{mn} = \sqrt{\frac{D}{\rho h}\frac{I_{1m}I_{2n} + 2I_{3m}I_{4n} + I_{6m}I_{5n}}{I_{6m}I_{2n}}} \tag{13}$$

Note that the adopted approach is computationally efficient since it leads to a diagonal system in the modal amplitude unknowns (see Eq. (6)), i.e., no explicit eigenvalue problem need to be solved for the unstiffened plate. As shown later, this diagonal structure will also be exploited to obtain a sparse eigenproblem for the ribbed plate. At the same time, the present formulation provides quite accurate upper bound solutions (an average error less than 0.5% in the natural frequencies), except when free edges and free corners are involved [17]. For this reason, only plates having various combinations of simply supported and clamped edges are considered in the following.

2.3. Stiffening beams

Forced bending and torsional motion of each y-wise stiffening beam can be written as follows [21]:

$$EI^i\frac{\partial^4 w^i}{\partial y^4} + \rho A^i\frac{\partial^2 w^i}{\partial t^2} = f^i \tag{14}$$

$$EI^i_w\frac{\partial^4 \theta^i}{\partial y^4} - GJ^i\frac{\partial^2 \theta^i}{\partial y^2} + \rho I^i_0\frac{\partial^2 \theta^i}{\partial t^2} = m^i \tag{15}$$

where $i = 1,2,\ldots,I$, $w^i = w^i(y,t)$ and $\theta^i = \theta^i(y,t)$ are transverse displacement and angle of twist, respectively, EI^i is the flexural rigidity, GJ^i refers to the Saint-Venant torsional rigidity for uniform torsion, EI^i_w denotes the warping rigidity associated with non-uniform warping, ρA^i is the mass per unit length, and ρI^i_0 is the mass moment of inertia per unit length. In a similar manner, forced bending and torsional motion of each jth x-wise beam can be written as follows:

$$EI^j\frac{\partial^4 w^j}{\partial x^4} + \rho A^j\frac{\partial^2 w^j}{\partial t^2} = f^j \tag{16}$$

$$EI^j_w\frac{\partial^4 \theta^j}{\partial x^4} - GJ^j\frac{\partial^2 \theta^j}{\partial x^2} + \rho I^j_0\frac{\partial^2 \theta^j}{\partial t^2} = m^j \tag{17}$$

where $j = 1,2,\ldots,J$, $w^j = w^j(x,t)$ and $\theta^j = \theta^j(x,t)$. Assuming time-harmonic motion, the solutions are sought to be

$$w^i = \sum_{n=1}^{N} w^i_n\psi_n(y)e^{j\omega t}, \quad \theta^i = \sum_{n=1}^{N}\theta^i_n\psi_n(y)e^{j\omega t} \tag{18a}$$

$$w^j = \sum_{m=1}^{M} w^j_m\phi_m(x)e^{j\omega t}, \quad \theta^j = \sum_{m=1}^{M}\theta^j_m\phi_m(x)e^{j\omega t} \tag{18b}$$

where w^i_n, θ^i_n, w^j_m and θ^j_m are the unknown modal amplitude of the corresponding mode. After substituting Eqs. (18a) into Eqs. (14) and (15), multiplying by the qth corresponding mode, integrating over the length b of the beam and using the orthogonality conditions, the solutions for the ith y-wise beam must satisfy the following modal equations:

$$\begin{aligned}(\kappa^i_{Bn} - \omega^2\mu^i_{Bn})w^i_n &= f^i_n \\ (\kappa^i_{Tn} - \omega^2\mu^i_{Tn})\theta^i_n &= m^i_n\end{aligned} \quad (n = 1,2,\ldots,N) \tag{19}$$

where

$$\kappa^i_{Bn} = EI^iI_{5n} \tag{20}$$

$$\mu^i_{Bn} = \rho A^iI_{2n} \tag{21}$$

are the modal stiffness and modal mass of the nth bending mode, respectively, and

$$\kappa_{Tn}^{i} = EI_{w}^{i} I_{5n} - GJ^{i} I_{4n} \tag{22}$$

$$\mu_{Tn}^{i} = \rho I_{0}^{i} I_{2n} \tag{23}$$

are the modal stiffness and modal mass of the nth torsional mode, respectively. With a similar procedure, the solutions for the jth x-wise beam must satisfy the following modal equations:

$$\begin{aligned} (\kappa_{Bm}^{j} - \omega^2 \mu_{Bm}^{j}) w_{m}^{j} &= f_{m}^{j} \\ (\kappa_{Tm}^{j} - \omega^2 \mu_{Tm}^{j}) \theta_{m}^{j} &= m_{m}^{j} \end{aligned} \quad (m = 1, 2, \ldots, M) \tag{24}$$

where

$$\kappa_{Bm}^{j} = EI^{j} I_{1m} \tag{25}$$

$$\mu_{Bm}^{j} = \rho A^{j} I_{6m} \tag{26}$$

are the modal stiffness and modal mass of the mth bending mode, respectively, and

$$\kappa_{Tm}^{j} = EI_{w}^{j} I_{1m} - GJ^{j} I_{3m} \tag{27}$$

$$\mu_{Tm}^{j} = \rho I_{0}^{j} I_{6m} \tag{28}$$

are the modal stiffness and modal mass of the mth torsional mode, respectively. The modal coupling loads in Eqs. (19) and (24) are given by the following expressions:

$$f_{n}^{i} = \int_{0}^{b} f^{i} \psi_{n} \, \mathrm{d}y, \quad m_{n}^{i} = \int_{0}^{b} m^{i} \psi_{n} \, \mathrm{d}y \tag{29a}$$

$$f_{m}^{j} = \int_{0}^{a} f^{j} \phi_{m} \, \mathrm{d}x, \quad m_{m}^{j} = \int_{0}^{a} m^{j} \phi_{m} \, \mathrm{d}x \tag{29b}$$

2.4. Ribbed plate

By comparing Eqs. (29a) and (29b) with Eqs. (7) and (8), one obtains the following relations between the modal coupling loads on the plate and those on the stiffening beams:

$$f_{mn} = -\sum_{i=1}^{I} \phi_{m}^{x_i} f_{n}^{i} - \sum_{j=1}^{J} \psi_{n}^{y_j} f_{m}^{j} \tag{30}$$

$$m_{mn} = -\sum_{i=1}^{I} \phi_{m}^{\prime x_i} m_{n}^{i} - \sum_{j=1}^{J} \psi_{n}^{\prime y_j} m_{m}^{j} \tag{31}$$

Then, using Eqs. (19) and (24), the harmonic motion of the plate can be written as follows:

$$\begin{aligned} (\kappa_{mn} - \omega^2 \mu_{mn}) w_{mn} = & -\sum_{i=1}^{I} \phi_{m}^{x_i} (\kappa_{Bn}^{i} - \omega^2 \mu_{Bn}^{i}) w_{n}^{i} - \sum_{j=1}^{J} \psi_{n}^{y_j} (\kappa_{Bm}^{j} - \omega^2 \mu_{Bm}^{j}) w_{m}^{j} \\ & - \sum_{i=1}^{I} \phi_{m}^{\prime x_i} (\kappa_{Tn}^{i} - \omega^2 \mu_{Tn}^{i}) \theta_{n}^{i} - \sum_{j=1}^{J} \psi_{n}^{\prime y_j} (\kappa_{Tm}^{j} - \omega^2 \mu_{Tm}^{j}) \theta_{m}^{j} \end{aligned} \tag{32}$$

Continuity conditions at the interface between the plate and the beams can be expressed as

$$w^{i} = w(x_i), \quad \theta^{i} = w'(x_i) \tag{33a}$$

$$w^{j} = w(y_j), \quad \theta^{j} = w'(y_j) \tag{33b}$$

According to the assumed solutions for the displacement of the plate and the displacement and rotation of the stiffening beams, the continuity conditions in Eqs. (33a) and (33b) can be rewritten in terms of modal amplitudes as follows:

$$w_n^i = \sum_{m=1}^{M} \phi_m^{x_i} w_{mn}, \quad \theta_n^i = \sum_{m=1}^{M} \phi_m^{\prime x_i} w_{mn} \tag{34a}$$

$$w_m^j = \sum_{n=1}^{N} \psi_n^{y_j} w_{mn}, \quad \theta_m^j = \sum_{n=1}^{N} \psi_n^{\prime y_j} w_{mn} \tag{34b}$$

By substituting Eqs. (34a) and (34b) into Eq. (32), the harmonic motion of the ribbed plate is described by the following set of coupled equations:

$$\begin{aligned}(\kappa_{mn} - \omega^2 \mu_{mn}) w_{mn} + \sum_{i=1}^{I} \sum_{p=1}^{M} [\phi_m^{x_i} (\kappa_{Bn}^i - \omega^2 \mu_{Bn}^i) \phi_p^{x_i} + \phi_m^{\prime x_i} (\kappa_{Tn}^i - \omega^2 \mu_{Tn}^i) \phi_p^{\prime x_i}] w_{pn} \\ + \sum_{j=1}^{J} \sum_{q=1}^{N} [\psi_n^{y_j} (\kappa_{Bm}^j - \omega^2 \mu_{Bm}^j) \psi_q^{y_j} + \psi_n^{\prime y_j} (\kappa_{Tm}^j - \omega^2 \mu_{Tm}^j) \psi_q^{\prime y_j}] w_{mq} = 0\end{aligned} \tag{35}$$

where p and q indexes denote the coupling terms due to the presence of the stiffening beams. Eq. (35) can be expressed in a standard matrix form as

$$(\mathbf{K} - \omega^2 \mathbf{M}) \mathbf{w} = \mathbf{0} \tag{36}$$

where the modal amplitudes are grouped into the column vector $\mathbf{w}$ as follows:

$$\mathbf{w} = [w_{11}, w_{12}, \ldots, w_{1N}, w_{21}, \ldots, w_{2N}, \ldots, w_{mn}, \ldots, w_{MN}]^{\mathrm{T}} \tag{37}$$

The mass matrix $\mathbf{M}$ is of the form

$$\begin{bmatrix} M_{1111} & M_{1112} & \cdots & M_{11pq} & \cdots & M_{11MN} \\ M_{1211} & M_{1212} & \cdots & & & \\ \vdots & & \ddots & & & \\ M_{mn11} & \cdots & & M_{mnpq} & & \\ \vdots & & & & \ddots & \\ M_{MN11} & & & & & M_{MNMN} \end{bmatrix} \tag{38}$$

whose elements are given by

$$\begin{aligned}M_{mnpq} = \mu_{mn} \delta_{mp} \delta_{nq} + \sum_{i=1}^{I} [\mu_{Bn}^i \phi_m^{x_i} \phi_p^{x_i} \delta_{nq} + \mu_{Tn}^i \phi_m^{\prime x_i} \phi_p^{\prime x_i} \delta_{nq}] \\ + \sum_{j=1}^{J} [\mu_{Bm}^j \psi_n^{y_j} \psi_q^{y_j} \delta_{mp} + \mu_{Tm}^j \psi_n^{\prime y_j} \psi_q^{\prime y_j} \delta_{mp}]\end{aligned} \tag{39}$$

where δ_{ij} is the Kronecker delta function. The stiffness matrix $\mathbf{K}$ is of the same size and form as $\mathbf{M}$. The elements of the stiffness matrix are given by

$$\begin{aligned}K_{mnpq} = \kappa_{mn} \delta_{mp} \delta_{nq} + \sum_{i=1}^{I} [\kappa_{Bn}^i \phi_m^{x_i} \phi_p^{x_i} \delta_{nq} + \kappa_{Tn}^i \phi_m^{\prime x_i} \phi_p^{\prime x_i} \delta_{nq}] \\ + \sum_{j=1}^{J} [\kappa_{Bm}^j \psi_n^{y_j} \psi_q^{y_j} \delta_{mp} + \kappa_{Tm}^j \psi_n^{\prime y_j} \psi_q^{\prime y_j} \delta_{mp}]\end{aligned} \tag{40}$$

Mass and stiffness matrices are real, symmetric, and positive definite. Further, as shown by Eqs. (39) and (40), they are sparse. The resulting sparse eigenproblem can be solved numerically in an efficient way using, for example, iterative projection methods of Arnoldi type. An algorithmic variant of the Arnoldi process called the Implicitly Restarted Arnoldi method is freely available within the FORTRAN package ARPACK [22]. The package is designed to compute a few L eigenvalues ω_l^2 and corresponding eigenvectors $\mathbf{w}_l$ with user specified features such as those of smallest magnitude. The ARPACK library is accessible in MATLAB via the built-in *eigs* command. Once the lth numerical eigenvector $\mathbf{w}_l$ is known, the lth natural mode shape of the ribbed plate may be recovered in the usual way as

$$w_l(x,y) = \mathbf{s}^{\mathrm{T}}\mathbf{w}_l \tag{41}$$

where

$$\mathbf{s} = [\phi_1\psi_1, \phi_1\psi_2, \ldots, \phi_1\psi_N, \phi_2\psi_1, \ldots, \phi_2\psi_N, \ldots, \phi_m\psi_n, \ldots, \phi_M\psi_N]^{\mathrm{T}} \tag{42}$$

2.5. Frequency equation for the single-ribbed plate

When the plate is stiffened by one single beam, the eigenproblem can be profitably put into an alternative form which provides an efficient method to solve for the eigenvalues of the ribbed structure. In this way, the frequency equation of the rib-stiffened plate may be derived in a compact form which can be easily coded and solved by any standard root solver routine.

Without any loss of generality, consider a plate stiffened by one single y-wise beam at location x_0. Eq. (35) reduce to the following:

$$(\kappa_{mn} - \omega^2\mu_{mn})w_{mn} + \sum_{p=1}^{M}[\phi_m^{x_0}(\kappa_{Bn} - \omega^2\mu_{Bn})\phi_p^{x_0} + \phi_m'^{x_0}(\kappa_{Tn} - \omega^2\mu_{Tn})\phi_p'^{x_0}]w_{pn} = 0 \tag{43}$$

These equations can be written concisely in matrix form as

$$[\mathbf{K}_p - \omega^2\mathbf{M}_p + \mathbf{U}_b(\mathbf{K}_b - \omega^2\mathbf{M}_b)\mathbf{U}_b^T + \mathbf{U}_t(\mathbf{K}_t - \omega^2\mathbf{M}_t)\mathbf{U}_t^T]\mathbf{w} = \mathbf{0} \tag{44}$$

where

$$\mathbf{U}_b = [\boldsymbol{\Phi}_1 \;\; \boldsymbol{\Phi}_2 \;\; \ldots \;\; \boldsymbol{\Phi}_M]^{\mathrm{T}} \tag{45}$$

$$\mathbf{U}_t = [\boldsymbol{\Phi}_1' \;\; \boldsymbol{\Phi}_2' \;\; \ldots \;\; \boldsymbol{\Phi}_M']^{\mathrm{T}} \tag{46}$$

$\boldsymbol{\Phi}_i$ and $\boldsymbol{\Phi}_i'$ are $N \times N$ diagonal matrices whose ith element is $\phi_i^{x_0}$ and $\phi_i'^{x_0}$, respectively. In Eq. (44) $\mathbf{K}_p$ and $\mathbf{M}_p$ are diagonal modal stiffness and mass matrices of the unstiffened plate whose elements are κ_{mn} and μ_{mn}, respectively; $\mathbf{K}_b$ and $\mathbf{M}_b$ are diagonal bending modal stiffness and mass matrices of the beam whose elements are κ_{Bn} and μ_{Bn}; and $\mathbf{K}_t$ and $\mathbf{M}_t$ are diagonal torsional modal stiffness and mass matrices of the beam whose elements are κ_{Tn} and μ_{Tn}. The natural frequencies of the ribbed plate are obtained by setting the determinant of the coefficient matrix of Eq. (44) equal to zero:

$$\det(\mathbf{K}_p - \omega^2\mathbf{M}_p + \mathbf{U}\mathbf{R}\mathbf{U}^{\mathrm{T}}) = 0 \tag{47}$$

where $\mathbf{U} = [\mathbf{U}_b \;\; \mathbf{U}_t]$ and the $2N \times 2N$ $\mathbf{R}$ matrix has the following block diagonal form:

$$\mathbf{R} = \begin{bmatrix} \mathbf{R}_b & \mathbf{0} \\ \mathbf{0} & \mathbf{R}_t \end{bmatrix} \tag{48}$$

where $\mathbf{R}_b = \mathbf{K}_b - \omega^2\mathbf{M}_b$ and $\mathbf{R}_t = \mathbf{K}_t - \omega^2\mathbf{M}_t$. According to the matrix determinant lemma [19], Eq. (47) can be expressed as

$$\det(\mathbf{K}_p - \omega^2\mathbf{M}_p)\det(\mathbf{I}_{2N} + \mathbf{R}\mathbf{U}^{\mathrm{T}}(\mathbf{K}_p - \omega^2\mathbf{M}_p)^{-1}\mathbf{U}) = 0 \tag{49}$$

where $\mathbf{I}_{2N}$ is the identity matrix of size $2N \times 2N$. Since the modal stiffness and mass matrices of the unstiffened plate are diagonal, Eq. (49) can also be written as

$$\prod_{m,n}(\kappa_{mn} - \omega^2\mu_{mn}) \det \mathbf{Z} = 0 \tag{50}$$

where the matrix $\mathbf{Z} = \mathbf{I}_{2N} + \mathbf{R}\mathbf{U}^{\mathrm{T}}(\mathbf{K}_p - \omega^2\mathbf{M}_p)^{-1}\mathbf{U}$ can be partitioned as

$$\mathbf{Z} = \begin{bmatrix} \mathbf{Z}_1 & \mathbf{Z}_2 \\ \mathbf{Z}_3 & \mathbf{Z}_4 \end{bmatrix} \tag{51}$$

The individual sub-matrices of Eq. (51) are as follows:

$$\mathbf{Z}_1 = \mathbf{I}_N + \mathbf{R}_b \sum_{m=1}^{M} \boldsymbol{\Phi}_m^{\mathrm{T}} \mathbf{P}_m^{-1} \boldsymbol{\Phi}_m \tag{52}$$

$$\mathbf{Z}_2 = \mathbf{R}_b \sum_{m=1}^{M} \boldsymbol{\Phi}_m^{\mathrm{T}} \mathbf{P}_m^{-1} \boldsymbol{\Phi}'_m \tag{53}$$

$$\mathbf{Z}_3 = \mathbf{R}_t \sum_{m=1}^{M} \boldsymbol{\Phi}_m'^{\mathrm{T}} \mathbf{P}_m^{-1} \boldsymbol{\Phi}_m \tag{54}$$

$$\mathbf{Z}_4 = \mathbf{I}_N + \mathbf{R}_t \sum_{m=1}^{M} \boldsymbol{\Phi}_m'^{\mathrm{T}} \mathbf{P}_m^{-1} \boldsymbol{\Phi}'_m \tag{55}$$

where $\mathbf{P}_m$ is a $N \times N$ diagonal matrix whose ith element is $\kappa_{mi} - \omega^2\mu_{mi}$. Note that all the sub-matrices are diagonal. Then, the characteristic determinant of Eq. (50) can be reduced to a simple frequency equation

Table 2
Convergence study of frequency parameters $\lambda = (\omega b^2/\pi^2)\sqrt{\rho h/D}$ for square SSSS and CCCC plates with one x-wise stiffening beam at $b/2$

	M, N	Mode sequence					
		1	2	3	4	5	6
SSSS plate with $h/b = 0.01$, $g/b = 0.01$, $t/h = 1.5$							
Present	3	2.1067	5.0093	5.7207	8.0237	9.8843	11.6035
	5	2.1066	5.0093	5.7145	8.0236	9.8839	11.5568
	7	2.1066	5.0093	5.7127	8.0236	9.8838	11.5426
	9	2.1066	5.0093	5.7120	8.0236	9.8837	11.5369
	11	2.1066	5.0093	5.7117	8.0235	9.8837	11.5342
	13	2.1066	5.0093	5.7115	8.0235	9.8837	11.5328
	15	2.1066	5.0093	5.7114	8.0235	9.8837	11.5320
Ref. [23]	15	2.1057	5.0090	5.7049	8.0219	9.8659	11.5174
NASTRAN		2.1008	5.0095	5.6604	8.0225	9.8870	11.4064
CCCC plate with $h/b = 0.01$, $g/b = 0.01$, $t/h = 1$							
Present	3	3.8138	7.4771	8.0913	11.0445	13.3384	14.6862
	5	3.8137	7.4771	8.0874	11.0444	13.3381	14.6629
	7	3.8136	7.4771	8.0862	11.0444	13.3381	14.6553
	9	3.8136	7.4771	8.0858	11.0444	13.3380	14.6524
	11	3.8136	7.4771	8.0855	11.0444	13.3380	14.6506
	13	3.8136	7.4771	8.0854	11.0444	13.3380	14.6498
	15	3.8136	7.4771	8.0853	11.0444	13.3380	14.6492
Ref. [23]	15	3.7947	7.4276	7.9970	10.9490	13.2376	14.4261
NASTRAN		3.7897	7.4426	7.9716	10.9777	13.2866	14.3817

of the form

$$\prod_{m,n}(\kappa_{mn}-\omega^2\mu_{mn})\prod_{n}(\zeta_{1n}\zeta_{4n}-\zeta_{2n}\zeta_{3n})=0 \tag{56}$$

where

$$\zeta_{1n}=1+(\kappa_{Bn}-\omega^2\mu_{Bn})\sum_{m=1}^{M}\frac{(\phi_m^{x_0})^2}{\kappa_{mn}-\omega^2\mu_{mn}} \tag{57}$$

$$\zeta_{2n}=(\kappa_{Bn}-\omega^2\mu_{Bn})\sum_{m=1}^{M}\frac{\phi_m^{x_0}\phi_m'^{x_0}}{\kappa_{mn}-\omega^2\mu_{mn}} \tag{58}$$

$$\zeta_{3n}=(\kappa_{Tn}-\omega^2\mu_{Tn})\sum_{m=1}^{M}\frac{\phi_m^{x_0}\phi_m'^{x_0}}{\kappa_{mn}-\omega^2\mu_{mn}} \tag{59}$$

Table 3
Convergence study of frequency parameters $\lambda=(\omega b^2/\pi^2)\sqrt{\rho h/D}$ for square SSSS and SCSC plates with multiple stiffening beams

BC		M,N	Mode sequence					
			1	2	3	4	5	6
Stiffening set (*b*): *one central y-wise and one central x-wise beam*								
SSSS	Present	5	2.2028	5.7225	5.7225	8.0472	11.2245	11.7234
		7	2.2027	5.7207	5.7207	8.0471	11.2147	11.7079
		9	2.2027	5.7200	5.7200	8.0470	11.2107	11.7018
		11	2.2027	5.7197	5.7197	8.0470	11.2087	11.6990
		13	2.2027	5.7195	5.7195	8.0470	11.2077	11.6975
		15	2.2027	5.7195	5.7195	8.0469	11.2071	11.6966
	Ref. [23]	15	2.2017	5.7167	5.7167	8.0552	11.1909	11.6785
	NASTRAN		2.1948	5.6684	5.6684	8.0495	11.1208	11.5956
SCSC	Present	5	3.3869	6.3886	8.1800	9.6658	12.3220	14.9087
		7	3.3866	6.3871	8.1738	9.6656	12.3098	14.9046
		9	3.3865	6.3865	8.1713	9.6656	12.3053	14.8947
		11	3.3864	6.3862	8.1702	9.6655	12.3024	14.8899
		13	3.3864	6.3860	8.1696	9.6655	12.3012	14.8874
		15	3.3864	6.3859	8.1693	9.6655	12.3001	14.8859
	Ref. [23]	15	3.3776	6.3094	8.1499	9.6347	12.0673	14.7993
	NASTRAN		3.3519	6.2591	8.0638	9.6389	11.9324	14.6904
Stiffening set (*c*): *two y-wise and two x-wise beams*								
SSSS	Present	5	2.2955	6.0273	6.0273	9.1625	12.6213	12.6216
		7	2.2954	6.0246	6.0246	9.1625	12.5799	12.5802
		9	2.2954	6.0244	6.0244	9.1603	12.5799	12.5801
		11	2.2954	6.0239	6.0239	9.1596	12.5726	12.5729
		13	2.2954	6.0237	6.0237	9.1596	12.5684	12.5687
		15	2.2954	6.0236	6.0236	9.1592	12.5684	12.5686
	Ref. [23]	15	2.2962	6.0185	6.0185	9.1513	12.5597	12.5599
	NASTRAN		2.2852	5.9544	5.9544	9.0638	12.3405	12.3440
SCSC	Present	5	3.5782	6.7428	8.6920	11.3996	12.9571	16.5930
		7	3.5776	6.7413	8.6830	11.3992	12.9345	16.5002
		9	3.5776	6.7410	8.6822	11.3937	12.9339	16.5001
		11	3.5775	6.7404	8.6804	11.3919	12.9254	16.4835
		13	3.5775	6.7402	8.6795	11.3918	12.9230	16.4742
		15	3.5775	6.7402	8.6793	11.3909	12.9229	16.4742
	Ref. [23]	15	3.5722	6.7223	8.6508	11.3273	12.9075	16.4203
	NASTRAN		3.5354	6.6518	8.5097	11.1700	12.7049	16.1271

$$\zeta_{4n} = 1 + (\kappa_{Tn} - \omega^2 \mu_{Tn}) \sum_{m=1}^{M} \frac{(\phi_m'^{x_0})^2}{\kappa_{mn} - \omega^2 \mu_{mn}} \tag{60}$$

Zeros of Eq. (56) can be determined either graphically or numerically using any standard root solver routine, such as *fzero* in MATLAB. The special form of the frequency equation (56) is significant because it reveals that, if the rib location coincides with a nodal line of any modes of the unstiffened plate, then some eigenvalues of the ribbed plate will be identical to those of the bare plate. Eq. (56) can be further simplified. When the rib location x_0 does not coincide with a nodal line of any of the modes of the unstiffened plate, then $\kappa_{mn} - \omega^2 \mu_{mn} \neq 0$. In this case, the frequency equation reduces to

$$\prod_n (\zeta_{1n}\zeta_{4n} - \zeta_{2n}\zeta_{3n}) = 0 \tag{61}$$

The above formulation takes into account both bending and torsion deformations of the stiffening beam. If the torsional contribution is negligible, Eq. (50) can be written as

$$\prod_{m,n} (\kappa_{mn} - \omega^2 \mu_{mn}) \det \mathbf{Z}_1 = 0 \tag{62}$$

which reduces to a simple frequency equation of the form

$$\prod_{m,n} (\kappa_{mn} - \omega^2 \mu_{mn}) \prod_n \zeta_{1n} = 0 \tag{63}$$

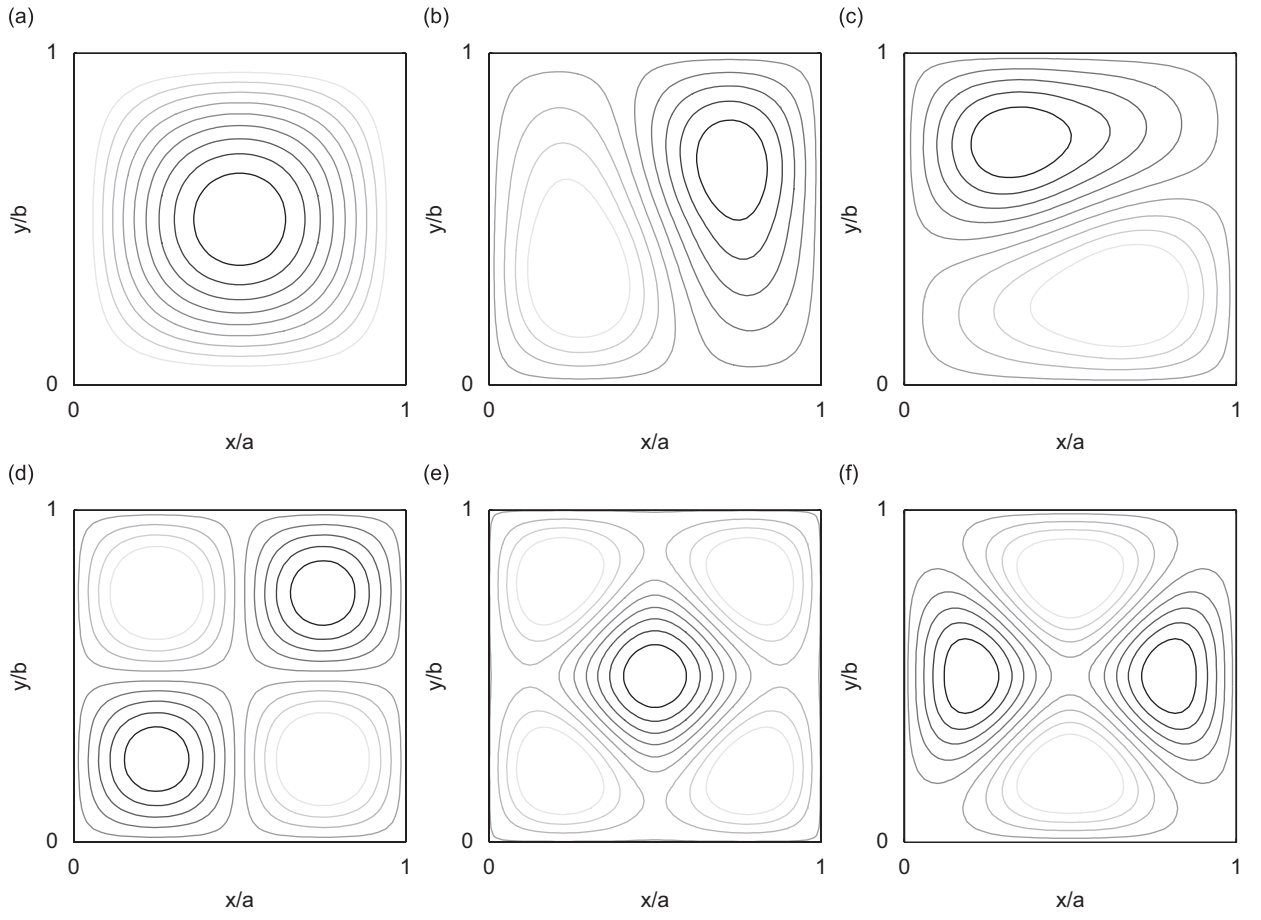

Fig. 2. Contours of vibration modes of a square SSSS plate with one central y-wise and one central x-wise beam. (a) First mode (2.2027); (b) second mode (5.7195); (c) third mode (5.7195); (d) fourth mode (8.0470); (e) fifth mode (11.2077); (f) sixth mode (11.6975).

where ζ_{1n} is given by Eq. (57). Finally, when the rib location x_0 does not coincide with a nodal line of any of the modes of the unstiffened plate, Eq. (63) simplifies further to give

$$\prod_n \zeta_{1n} = 0 \tag{64}$$

3. Numerical results and discussion

The accuracy and applicability of the formulation presented in this work is first examined by studying the convergence of the method on square ribbed plates having various boundary conditions. In the following analysis, we shall use the letters S for simply supported edge and C for clamped edge and the usual four-letter designation to represent the edge conditions of the plate. For instance, an SCSC plate will have edges 1–2 and 3–4 simply supported and edges 2–3 and 4–1 clamped (see Fig. 1). The dimensionless frequency parameters, $\lambda = (\omega b^2/\pi^2)\sqrt{\rho h/D}$, will be presented. Three different types of stiffening set are considered: (a) one central x-wise beam, (b) one central y-wise and one central x-wise beam, and (c) two equally spaced y-wise and two equally spaced x-wise beams. It is also assumed that all stiffeners have the same rectangular cross-section of width g and depth t (see Fig. 1). Poisson's ratio $\nu = 0.3$ and a plate thickness ratio $h/b = 0.01$ are used throughout this study.

Results obtained using the method developed here are compared with the Ritz results published by Liew et al. [23] and those obtained using a standard FEM analysis. Liew et al. solved the free vibration problem

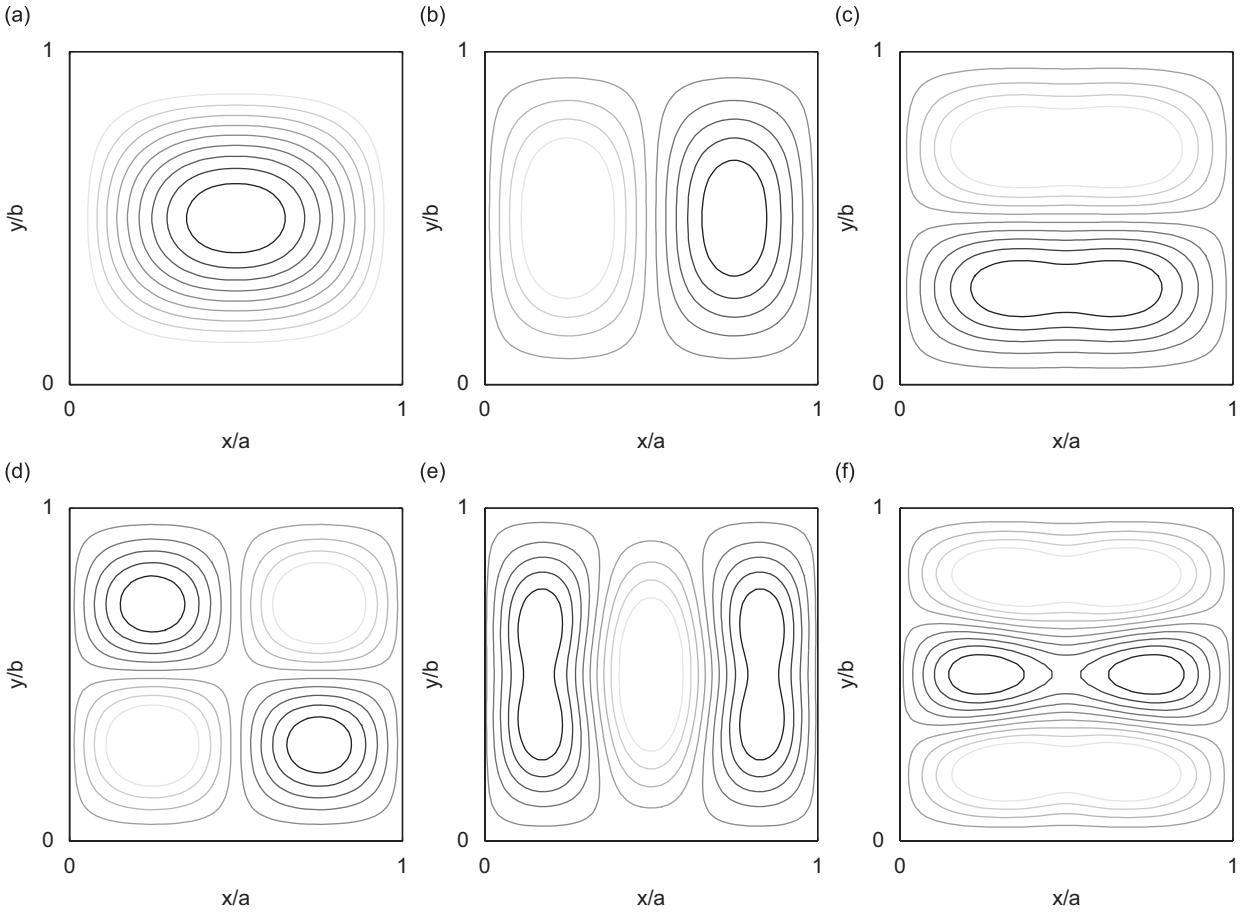

Fig. 3. Contours of vibration modes of a square SCSC plate with one central y-wise and one central x-wise beam. (a) First mode (3.3864); (b) second mode (6.3860); (c) third mode (8.1696); (d) fourth mode (9.6655); (e) fifth mode (12.3012); (f) sixth mode (14.8874).

using the Ritz method with mathematically complete algebraic polynomials with a degree set of 15. They used Mindlin theory to model the plate and Timoshenko theory to model the stiffeners, whereas in-plane displacements of the plate and warping stiffness of the beams were neglected in their formulation. FEM analysis was carried out with NASTRAN using 7500 four-node isoparametric CQUAD4 flat elements to model the plate and 50 CBEAM elements to model each stiffening beam. Both membrane and bending behavior is included in the shell element formulation. Contribution of transverse shear deformation and cross-section warping to torsional stiffness are included in the beam element formulation. Eccentricity of the stiffeners is modeled through the offset modeling feature of the beam element and mass lumping is used in the eigenvalue analysis. Comparison with results obtained by the two reference models can give information on how the accuracy of the present method is influenced by the different assumptions of the formulation. The accuracy of the single-term solution for the plate and the effect of shear deformation of the plate and stiffeners can be evaluated by comparison with results published by Liew et al. The importance of in-plane displacements can be predicted by further comparisons between the present approach and FEM analysis.

Table 2 gives the first six frequency parameters versus the number $M = N$ of mode shape functions used in the model for single-ribbed (stiffening set (a)) SSSS and CCCC square plates with different t/h ratios and a fixed stiffener width ratio $g/b = 0.01$. Present results have been obtained using the frequency equation (56). From Table 2 it can be seen that the six frequency parameters converge monotonically from above with the increase of the number of beam functions used in the assumed solution. As expected, the present formulation provides upper bound values for the natural frequencies. Results also show that the solution for the first

Table 4
Comparison study of frequency parameters $\lambda = (\omega b^2/\pi^2)\sqrt{\rho h/D}$ for rectangular plates ($a/b = 2$) with different boundary conditions (BC) and stiffening set

BC	t/h		Mode sequence					
			1	2	3	4	5	6
Stiffening set (*a*): *one central x-wise beam*								
SSSS	1	Present	1.2435	2.0379	3.3941	4.2512	5.0045	5.3040
		Ref. [23]	1.2432	2.0372	3.3919	4.2483	5.0010	5.2989
	1.5	Present	1.2457	2.1066	3.6067	4.2524	5.0093	5.7115
		Ref. [23]	1.2454	2.1057	3.6041	4.2507	5.0090	5.7060
SCSC	1	Present	2.3873	2.9513	4.1096	5.9104	6.4386	7.0320
		Ref. [23]	2.3852	2.9439	4.0854	5.8552	6.4276	7.0172
	1.5	Present	2.3781	3.0022	4.3262	6.3773	6.4396	7.0373
		Ref. [23]	2.3760	2.9938	4.2947	6.2988	6.4301	7.0263
CCCC	1	Present	2.4853	3.3073	4.7913	6.5034	6.9176	7.2426
		Ref. [23]	2.4775	3.2908	4.7571	6.4730	6.8481	7.1940
	1.5	Present	2.4966	3.4344	5.1352	6.5048	7.2487	7.5347
		Ref. [23]	2.4897	3.4165	5.0883	6.4757	7.2035	7.4317
Stiffening set (*c*): *two y-wise and two x-wise beams*								
SSSS	1	Present	1.2992	2.0845	3.4689	4.4657	5.1837	5.4341
		Ref. [23]	1.2990	2.0840	3.4677	4.4627	5.1801	5.4291
	1.5	Present	1.3852	2.2291	3.7852	4.7950	5.4760	6.0493
		Ref.[23]	1.3855	2.2296	3.7863	4.7935	5.4764	6.0444
SCSC	1	Present	2.5411	3.0777	4.1455	6.0176	6.7364	7.2821
		Ref. [23]	2.5387	3.0713	4.1283	5.9881	6.7250	7.2693
	1.5	Present	2.7426	3.3015	4.4135	6.6563	7.1881	7.6484
		Ref. [23]	2.7404	3.2969	4.4024	6.6374	7.1780	7.6403
CCCC	1	Present	2.6374	3.4660	4.8544	6.8068	7.0342	7.6675
		Ref. [23]	2.6315	3.4474	4.8306	6.7908	7.0014	7.5801
	1.5	Present	2.8552	3.8090	5.2872	7.2543	7.8368	8.2815
		Ref. [23]	2.8528	3.7893	5.2683	7.2651	7.8194	8.1636

modes is well converged with acceptable accuracy when $M = N = 9$. More terms ($M = N = 13$) are needed to provide accurate results for the higher modes.

The same conclusions can be drawn from Table 3 which gives the first six frequency parameters versus the degree set $M = N$ for SSSS and SCSC square plates having multiple stiffeners (stiffening set (b) and (c)). Results are presented for a stiffener width ratio $g/b = 0.01$ and a stiffener height ratio $t/h = 1.5$. Thus, $M = N = 13$ is sufficient to guarantee good convergence of the method with acceptable accuracy for the number of modes included in the present analysis.

A closer look at the results of Tables 2 and 3 indicates that the solutions generated using the present combined analytical–numerical method are in close agreement with those obtained by Liew et al. The difference between the upper bound values is less than 0.1% for SSSS plates and, as discussed above, it may be attributed to the shear deformation included in the model of Ref. [23]. For plates with boundary conditions other than simply supported, the difference is slightly higher (less than 1%) due to the added approximation of the single-term solution. Good agreement is also observed with FEM results. Inclusion of in-plane displacements reveals that deviations between 1% and 2% occur in most cases. Such an accuracy is generally acceptable for many industrial applications during the preliminary design process. Isolated examples of very small errors are the second and fourth mode in Table 2 and the fourth mode in Table 3 for the stiffening set (b). This different behavior can be explained by looking at the mode shapes of the ribbed plate. Contour plots of the first six mode shapes for the SSSS and SCSC plates of Table 3 are shown in Figs. 2 and 3, respectively. Significant deformation of the stiffeners takes place in all modes, except for the fourth mode where the stiffeners does not deform at all in both cases. Thus, inclusion of in-plane displacement has little influence on this modes.

A comparison study on the first six frequency parameters is given in Table 4 for rectangular ribbed plates with aspect ratio $a/b = 2$. Two stiffening set (a) and (c) with increasing stiffener height ratio t/h and a fixed width ratio $g/b = 0.01$ are considered. Three boundary conditions, SSSS, SCSC, and CCCC, are studied for

Table 5
Frequency parameters $\lambda = (\omega b^2/\pi^2)\sqrt{\rho h/D}$ for square and rectangular CSSS ribbed plates with $g/b = 0.01$

a/b	t/h	Mode sequence					
		1	2	3	4	5	6
Stiffening set (*a*): *one central x-wise beam*							
1	1	2.4948	5.2749	6.3520	8.7520	10.1475	12.3302
	1.5	2.6357	5.2802	6.8682	8.7640	10.1378	13.1801
	2	2.8514	5.2857	7.5193	8.7764	10.1529	13.9507
2	1	1.3180	2.2477	3.7531	4.3009	5.1326	5.8094
	1.5	1.3304	2.3496	4.0154	4.3023	5.1377	6.2720
	2	1.3544	2.5101	4.3038	4.3955	5.1429	6.5095
Stiffening set (*b*): *one central y-wise and one central x-wise beam*							
1	1	2.5175	5.5707	6.3491	8.7850	10.8817	12.2481
	1.5	2.7040	5.9738	6.8689	8.8564	11.6341	13.1323
	2	2.9882	6.5076	7.5302	8.9756	12.3583	14.0372
2	1	1.3558	2.2515	3.7510	4.4779	5.1633	5.8086
	1.5	1.4221	2.3595	4.0220	4.6582	5.2231	6.2730
	2	1.5259	2.5287	4.4197	4.8104	5.3223	6.8835
Stiffening set (*c*): *two y-wise and two x-wise beams*							
1	1	2.5718	5.6941	6.4912	9.2921	11.3505	12.8066
	1.5	2.8357	6.3275	7.2809	10.1615	12.7396	14.4217
	2	3.2237	7.2392	8.3978	11.4094	14.4897	16.4111
2	1	1.3731	2.3022	3.8459	4.5149	5.3368	5.9687
	1.5	1.4685	2.4909	4.2387	4.8436	5.6537	6.6769
	2	1.6156	2.7759	4.8092	5.3164	6.0811	7.3795

each stiffening set and t/h ratio. It is shown that the frequency parameters generated from this study agree well with the results from Ref. [23] for all cases considered. The present results are only slightly higher when compared with those obtained by Liew et al.

It has to be noted that the method developed here is limited by the main assumptions made earlier in the formulation where the beam/plate interface is treated as a line contact and the plate bending–membrane coupling is neglected. Good agreement of the present results with other approaches confirms the validity of the proposed method for a stiffener width ratio $g/b = 0.01$ and a stiffener height ratio $t/h = 1$ and 1.5. It is found that when the beam width is not greater than the plate thickness the stiffener can be considered to be narrow and the line connection assumption is valid. In addition, low height ratios t/h imply light stiffeners when compared to the weight of the plate and, therefore, less coupling between out-of-plane and in-plane displacements of the plate for those modes where significant deformation of the stiffeners takes place. A poorer accuracy is expected with increasing the ratio between stiffener cross-sectional area and the cross-sectional area of the plate between stiffeners.

The computational advantage of the approach developed here can be exploited to gather useful and rapid information about the effects of geometry and boundary conditions on the natural frequencies of the ribbed plate without resorting to cumbersome FEM analysis. As shown earlier, the accuracy of the method is acceptable during the preliminary design process. As an example of the feasibility of the present formulation, new results for CSSS, CCSS, and CCCS ribbed plates with different stiffening sets, plate aspect ratios a/b and stiffener height ratios t/h are presented in Tables 5–7. It can be observed that the frequency parameters decrease with increasing a/b ratio, increase with higher constraint, from simply supported to clamped, at the four edges and increase with increasing t/h ratio.

Note that the present method can be applied to plates stiffened by beams with any symmetrical cross-section. It can also be extended to plates with arbitrary orientation of stiffeners by considering a local

Table 6
Frequency parameters $\lambda = (\omega b^2/\pi^2)\sqrt{\rho h/D}$ for square and rectangular CCSS ribbed plates with $g/b = 0.01$

a/b	t/h	Mode sequence					
		1	2	3	4	5	6
Stiffening set (*a*): *one central x-wise beam*							
1	1	2.8348	6.1836	6.5859	9.4863	11.5971	12.5301
	1.5	2.9619	6.1943	7.0909	9.5777	11.5799	13.2956
	2	3.1601	6.2124	7.6924	9.7545	11.5809	13.8202
2	1	1.8010	2.6136	4.0415	5.3145	6.0558	6.0569
	1.5	1.8064	2.7025	4.2930	5.3124	6.0628	6.5102
	2	1.8209	2.8459	4.6575	5.3106	6.0746	7.0830
Stiffening set (*b*): *one central y-wise and one central x-wise beam*							
1	1	2.9076	6.5806	6.5936	9.5359	12.4026	12.5109
	1.5	3.1441	7.0643	7.1406	9.7130	13.0512	13.4680
	2	3.4989	7.6045	7.8683	10.0301	13.5847	14.3491
2	1	1.8694	2.6220	4.0548	5.5295	6.0581	6.0987
	1.5	1.9664	2.7241	4.3356	5.7062	6.1825	6.5163
	2	2.1106	2.8888	4.7475	5.8246	6.3094	7.0977
Stiffening set (*c*): *two y-wise and two x-wise beams*							
1	1	2.9717	6.7397	6.7397	10.1081	12.9871	12.9880
	1.5	3.2975	7.5480	7.5484	11.1287	14.5761	14.5801
	2	3.7719	8.6916	8.6928	12.5553	16.5092	16.5166
2	1	1.8976	2.7000	4.1267	5.5879	6.2106	6.3128
	1.5	2.0419	2.9170	4.5030	5.9820	6.6629	6.9120
	2	2.2610	3.2429	5.0566	6.5309	7.0897	7.9015

Table 7
Frequency parameters $\lambda = (\omega b^2/\pi^2)\sqrt{\rho h/D}$ for square and rectangular CCCS ribbed plates with $g/b = 0.01$

a/b	t/h	Mode sequence					
		1	2	3	4	5	6
Stiffening set (*a*): *one central x-wise beam*							
1	1	3.3918	6.4597	7.7556	10.3308	11.7969	14.2321
	1.5	3.6145	6.4820	8.3475	10.4670	11.8092	14.9665
	2	3.9388	6.5215	8.9503	10.7407	11.8599	15.3730
2	1	1.8696	2.8348	4.4200	5.3473	6.1836	6.5859
	1.5	1.8894	2.9619	4.7244	5.3460	6.1943	7.0909
	2	1.9268	3.1601	5.1502	5.3456	6.2124	7.6632
Stiffening set (*b*): *one central y-wise and one central x-wise beam*							
1	1	3.4532	6.9252	7.7610	10.3463	12.8516	14.1363
	1.5	3.7782	7.5582	8.3589	10.4979	13.9345	15.0211
	2	4.2557	8.4027	8.9724	10.7843	14.7835	16.0153
2	1	1.9491	2.8368	4.4304	5.6191	6.1869	6.5883
	1.5	2.0770	2.9658	4.7637	5.8933	6.2012	7.0958
	2	2.2696	3.1656	5.2360	6.1614	6.2230	7.7006
Stiffening set (*c*): *two y-wise and two x-wise beams*							
1	1	3.5316	7.0523	7.9288	11.1131	13.1695	14.8191
	1.5	3.9598	7.9171	8.9261	12.3814	14.7553	16.6013
	2	4.5732	9.1337	10.3265	14.1481	16.6319	18.6189
2	1	1.9674	2.9391	4.5225	5.6266	6.5462	6.7657
	1.5	2.1265	3.2200	4.9736	6.0255	7.0781	7.5611
	2	2.3662	3.6358	5.6260	6.5726	7.8074	8.4840

coordinate system for each stiffening beam and introducing in Eqs. (33a) and (33b) a coordinate transformation between this local coordinate system and the global coordinate system of the plate.

4. Conclusions

An easy to code and computationally efficient analytical–numerical method for quick prediction of the eigenpairs of rib-stiffened plates is presented. The approach results in a sparse generalized eigenvalue problem that can be profitably solved by reliable methods to calculate only a small set of selected eigenmodes. An alternative formulation is also proposed for the single-ribbed case. A compact form of the frequency equation is derived whose solution can be easily determined either graphically or numerically. The extent and limits of validity of the present method are presented by comparison with published results and standard finite element analysis.

References

[1] S.F. Ney, G.G. Kulkarni, On the transverse free vibration of beam-slab type highway bridges, *Journal of Sound and Vibration* 21 (1972) 249–261.
[2] T. Balendra, N.E. Shanmugam, Free vibration of plate structures by grillage method, *Journal of Sound and Vibration* 99 (1985) 333–350.
[3] E.H. Dowell, Free vibrations of an arbitrary structure in terms of component modes, *Journal of Applied Mechanics* 39 (1972) 727–732.
[4] K.M. Liew, Y. Xiang, S. Kitipornchai, J.L. Meek, Formulation of Mindlin–Engesser model for stiffened plate vibration, *Computer Methods in Applied Mechanics and Engineering* 120 (3–4) (1995) 339–353.
[5] A. Berry, C. Locqueteau, Vibration and sound radiation of fluid-loaded stiffened plates with consideration of in-plane deformation, *Journal of the Acoustical Society of America* 100 (1) (1996) 312–319.

[6] G. Asku, R. Ali, Free vibration analysis of stiffened plates using finite difference method, *Journal of Sound and Vibration* 48 (1976) 15–25.
[7] A. Mukherjee, M. Mukhopadhyay, Finite element free vibration of eccentrically stiffened plates, *Computers and Structures* 30 (1988) 1303–1317.
[8] A. Bhimaraddi, A.J. Carr, P.J. Moss, Finite element analysis of laminated shells of revolution with laminated stiffeners, *Computers and Structures* 33 (1989) 295–305.
[9] I.E. Harik, M. Guo, Finite element analysis of eccentrically stiffened plates in free vibration, *Computers and Structures* 49 (1993) 1007–1015.
[10] H. Zeng, C.W. Bert, A differential quadrature analysis of vibration for rectangular stiffened plates, *Journal of Sound and Vibration* 241 (2001) 247–252.
[11] L.X. Peng, K.M. Liew, S. Kitipornchai, Buckling and free vibration analyses of stiffened plates using the FSDT mesh-free method, *Journal of Sound and Vibration* 289 (2006) 421–449.
[12] M. Petyt, Finite strip analysis of flat skin-stringer structures, *Journal of Sound and Vibration* 54 (1977) 537–547.
[13] M. Mukhopadhyay, Vibration and stability analysis of stiffened plates by semi-analytical finite difference method—part I: consideration of bending displacements only, *Journal of Sound and Vibration* 130 (1989) 27–39.
[14] J.S. Wu, S.S. Luo, Use of the analytical-and-numerical-combined method in the free vibration analysis of a rectangular plate with any number of point masses and translation springs, *Journal of Sound and Vibration* 200 (1997) 179–194.
[15] P.D. Cha, A general approach to formulating the frequency equation for a beam carrying miscellaneous attachments, *Journal of Sound and Vibration* 286 (2005) 921–939.
[16] J.N. Reddy, *Energy Principles and Variational Methods in Applied Mechanics*, second ed., Wiley, New Jersey, 2002.
[17] A.W. Leissa, The free vibration of rectangular plates, *Journal of Sound and Vibration* 31 (1973) 257–293.
[18] G.B. Warburton, The vibration of rectangular plates, *Proceedings of the Institute of Mechanical Engineers, Series A* 168 (1954) 371–384.
[19] H.V. Henderson, S.R. Searle, On deriving the inverse of a sum of matrices, *SIAM Review* 23 (1981) 53–60.
[20] P.D. Cha, N.C. Yoder, Applying Sherman–Morrison–Woodbury formulas to analyze the free and forced responses of a linear structure carrying lumped elements, *Journal of Vibration and Acoustics* 129 (2007) 307–316.
[21] S.S. Rao, *Vibration of Continuous Systems*, Wiley, Hoboken, 2007.
[22] R.B. Lehoucq, D.C. Sorensen, C. Yang, *ARPACK Users' Guide: Solution of Large-Scale Eigenvalue Problems with Implicitly Restarted Arnoldi Methods*, SIAM Publications, Philadelphia, 1998.
[23] K.M. Liew, Y. Xiang, S. Kitipornchai, M.K. Lim, Vibration of rectangular Mindlin plates with intermediate stiffeners, *Journal of Vibration and Acoustics* 116 (1994) 529–535.